

Phase Diagram of Diluted Magnetic Semiconductor Quantum Wells

L. Brey and F. Guinea

Instituto de Ciencia de Materiales (CSIC), Cantoblanco, 28049 Madrid, Spain

(Received 12 April 2000)

The phase diagram of diluted magnetic semiconductor quantum wells is investigated. The interaction between the carriers in the hole gas can lead to first-order ferromagnetic transitions, which remain abrupt in applied fields. These transitions can be induced by magnetic fields or, in double-layer systems, by electric fields. We make a number of precise experimental predictions for observing these first-order phase transitions.

PACS numbers: 75.50.Pp, 73.61.Ey, 75.70.Cn

Semiconductor and ferromagnetic materials have complementary properties in information processing and storage technologies [1]. Recent advances in the molecular-beam epitaxy growing techniques have made possible the fabrication of Mn-based diluted magnetic semiconductors (DMS) with a rather high ferromagnetic-paramagnetic critical temperature T_c [2]. In semiconductors it is possible to modulate spatially the density of carriers by changing the doping profiles but in DMS it is also suitable to vary the magnetic order of the carriers by changing the magnetic ion densities. The combination of these two possibilities opens a rich field of applications for these materials.

The high critical temperature DMS's have a high concentration, c , of Mn^{2+} ions, randomly located. The itinerant carriers in the $\text{Ga}_{1-x}\text{Mn}_x\text{As}$ systems are holes, and their density, c^* , is much smaller than the magnetic ion density. In a doped semiconductor the spin $S = 5/2$ Mn^{2+} ions feel a long range ferromagnetic interaction created by the coupling mediated by the itinerant spin polarized carriers [3–6]. This interaction has some resemblance to the one observed in the pyrochlores [7,8], where a similar type of coupling between a narrow electronic band and magnetic ions is assumed to exist. In the latter case, the phase diagram is significantly different from that of a conventional itinerant ferromagnet, showing first-order transitions and phase separation [9] and/or the formation of localized textures near the transition temperature [10]. These features lead to interesting transport properties, like colossal magnetoresistance. We expect these effects to be amplified in low density two-dimensional (2D) doped semiconductors, where the carrier-carrier interaction can play a significant role and also favors ferromagnetism [11].

In this work, we investigate the nature of the phase diagram of diluted magnetic semiconductor quantum wells, with an emphasis on the existence of abrupt transitions for experimentally accessible parameters. We analyze quantum wells made of GaMnAs growth in the $\langle 001 \rangle$ direction and with thickness w . The confinement of the carriers in the z direction can be obtained by sandwiching

the GaMnAs system between nonmagnetic GaAlAs semiconductors.

The system is described by the following Hamiltonian:

$$\mathcal{H} = g_I \mu_B \mathbf{B} \sum_I \mathbf{S}_I + \mathcal{H}_h + J \sum_{I,i} \mathbf{S}_I \cdot \mathbf{s}_i \delta(\mathbf{r}_i - \mathbf{R}_I). \quad (1)$$

We now analyze the three terms contributing to \mathcal{H} .

(i) $g_I \mu_B \mathbf{B} \sum_I \mathbf{S}_I$ is the Zeeman coupling between the localized spins and an external magnetic field B . Direct interactions between the magnetic moments of the Mn ions are much smaller than the interaction with the carrier spins [12] and therefore we neglect this coupling.

(ii) \mathcal{H}_h is the part of the Hamiltonian which describes the itinerant holes. It is the sum of the kinetic energy of the holes and the hole-hole interaction energy. We treat the kinetic energy of the carriers in the framework of the envelope function approximation. The confinement of the carriers in the quantum well produces the quantization of their motion and the appearance of subbands which, for sufficiently narrow quantum wells, have a clear light-hole or heavy-hole character. We assume that the hole density is low enough so that only one of the subbands, heavylike, is occupied. With this, the in plane motion of the holes can be approximated by a single parabolic band of effective mass m^* . We describe the interaction between the electrical carriers with the local spin density approximation (LSDA) [13]. Except at very low densities, the LSDA gives an accurate description of the electron gas confined in quantum wells [14,15].

(iii) The last term is the antiferromagnetic exchange interaction between the spin of the Mn^{2+} ions located at \mathbf{R}_I and the spins, $\tilde{\mathbf{s}}_i$, of the itinerant carriers. The interaction between ions mediated by the conduction holes is of long range. Thus we will assume that thermal distribution of the orientation of the Mn spins is that induced by an effective field, due to the holes, which should be calculated self-consistently.

Since the hole g factor is much smaller than that of Mn we neglect the coupling between $\tilde{\mathbf{s}}_i$ and B .

The aim of this work is to study the magnetic phase diagram of DMS quantum wells with a 2D density of holes $n_{2D} = c^*w$. For doing that we write the free energy \mathcal{F} as a function of the carrier spin polarization, $\xi = \frac{n_{\uparrow} - n_{\downarrow}}{n_{2D}}$, which is the order parameter. Here n_{σ} is the 2D density of carriers with spin σ . The critical temperatures for the ferromagnetic to paramagnetic transition in DMS is typically smaller than 100 K, and for these temperatures we can consider that the electron gas is degenerate [16]. Hence, the only temperature dependence in \mathcal{F} is due to thermal fluctuations of the Mn spins. Treating the holes in the LSDA the free energy per unit area takes the form

$$\mathcal{F} = \mathcal{F}_{\text{ions}} + \frac{\hbar^2}{m^*} \frac{\pi}{2} n_{2D}^2 (1 + \xi^2) + E_{\text{xc}}(n_{2D}, \xi). \quad (2)$$

Here E_{xc} is the hole exchange correlation energy and $\mathcal{F}_{\text{ions}}$ is the contribution of ion spins to the free energy:

$$\mathcal{F}_{\text{ions}} = -Tcw \log \frac{\sinh[h(S + 1/2)/T]}{\sinh(h/2T)}, \quad (3)$$

$$\text{with } h = \frac{J}{2} \frac{n_{2D}}{w} \xi + g_I \mu_B B. \quad (4)$$

In obtaining Eq. (3) we have assumed that the hole wave function in the z direction has the form $w^{-1/2}$.

The phase diagram with parameters $J = 0.15 \text{ eV nm}^3$, ion concentration $c = 1 \text{ nm}^{-3}$ and $w = 10 \text{ nm}$, is shown in Fig. 1. We include a single hole band of effective mass $m_{\parallel} = 0.11m_e$ and a dielectric constant $\epsilon_0 = 12.2$ [6]. We use the expression given by Vosko *et al.* [13] for E_{xc} .

The phase diagram is obtained by minimizing the free energy Eq. (2) with respect to ξ , for different values of T . A finite value of ξ indicates a ferromagnetic state whereas $\xi = 0$ corresponds to the paramagnetic phase. An abrupt/continuous change, as a function of T , in the value of ξ is the mark of a first-/second-order transition. In the high density region, the dashed line which represents the second-order phase transition agrees with that obtained from the divergences of the magnetic susceptibility [6]. The main novelty of our calculation is the identification of a first-order transition to a fully polarized state at intermediate densities. This transition takes place at higher T than that at which the magnetic susceptibility of the system diverges. The existence of a first-order transition between the paramagnetic and the ferromagnetic phases implies that, if the chemical potential is kept fixed, the carrier density will change abruptly. Conversely, if the average hole density is fixed, a region where inhomogeneous solutions are stable will appear near the transition, leading to phase separation. At higher densities, when a continuous transition between $\xi = 0$ and $\xi \neq 0$ occurs, we also find a

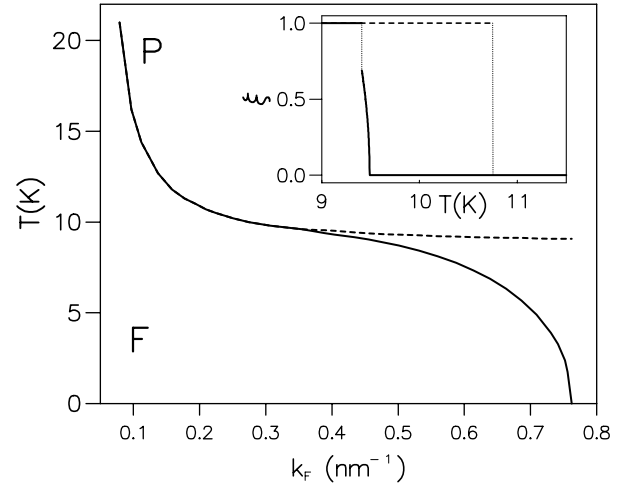


FIG. 1. Phase diagram of a DMS quantum well, using the parameters described in the text. Full and broken lines represent first- and second-order phase transitions, respectively, between ferromagnetic (F) and paramagnetic (P) phases. In the inset we show the carrier spin polarization for two different densities. The broken line corresponds to $k_F = 0.2 \text{ nm}^{-1}$, in this case there is a first-order transition between the $\xi = 1$ ferromagnetic phase and the paramagnetic phase. The continuous line corresponds to $k_F = 0.39 \text{ nm}^{-1}$. Upon lowering the temperature we obtain a continuous transition between the P and the F phases followed by an abrupt transition between two F phases with different values of ξ . As commented in the text, this last transition is probably spurious.

first-order phase transition between the partially polarized system, $\xi < 1$, and the fully polarized phase, $\xi = 1$. As we comment below we believe that this is a spurious transition related to the LSDA.

In order to understand better the phase diagram it is illustrative to derive the existence of these first-order transitions analytically. For doing that we treat the hole-hole interaction in the Hartree-Fock (HF) approximation. We obtain that the HF results are in rather good agreement with those obtained using the LSDA. In the HF approach the hole energy per unit area can be written as, [17]

$$E_{\text{holes}} = \frac{\hbar^2}{m^*} \frac{\pi}{2} n_{2D}^2 (1 + \xi^2) - \frac{3}{8\pi} \frac{e^2}{\epsilon_0} \left(\frac{3\pi^2}{w} \right)^{1/3} \times n_{2D}^{4/3} [(1 + \xi)^{4/3} + (1 - \xi)^{4/3}], \quad (5)$$

where the last term is the exchange energy of the holes. The free energy of the ions is given by Eq. (3). Near a paramagnetic-ferromagnetic transition, the hole spin polarization is small and we can expand the total free energy in terms of powers of ξ :

$$\mathcal{F}_{\text{tot}} \approx \frac{\hbar^2}{m^*} \frac{\pi}{2} n_{2D}^2 - C_1 \frac{3}{4} \frac{n_{2D}^{4/3}}{w^{1/3}} - Tcw \log(2S + 1) + \xi^2 \left[\frac{\hbar^2}{m^*} \frac{\pi}{2} n_{2D}^2 - C_1 \frac{1}{6} \frac{n_{2D}^{4/3}}{w^{1/3}} - \frac{1}{T} \frac{c}{w} \frac{S(S+1)}{24} J^2 n_{2D}^2 \right] + \xi^4 \left[-C_1 \frac{5}{324} \frac{n_{2D}^{4/3}}{w^{1/3}} + \frac{1}{T^3} \frac{c}{w^3} \frac{J^4 n_{2D}^4}{16} \left[\frac{7}{360} \left(S + \frac{1}{2} \right)^4 - \frac{S^2(S+1)^2}{72} \right] \right] + \dots, \quad (6)$$

with $C_1 = (\frac{3}{\pi})^{1/3} \frac{e^2}{\epsilon_0}$.

We expect a paramagnetic-ferromagnetic transition when the quadratic term in ξ is zero. This implies

$$T_c = \frac{1}{12w} \frac{cJ^2S(S+1)}{\pi \frac{\hbar^2}{m^*} - \frac{1}{3\pi} \frac{e^2}{\epsilon_0} (\frac{3\pi^2}{w})^{1/3} n_{2D}^{-2/3}}. \quad (7)$$

At high densities, this approximation gives $T_c \approx 8.7$ K, in good agreement with the LSDA calculation and with the RKKY solution [6]. Note that the only dependence of T_c on n_{2D} is through the hole-hole interaction. This is due to the fact that the two-dimensional density of states is energy independent. In three-dimensional systems the kinetic energy scales as $n^{5/3}$ and T_c is proportional to $n^{1/3}$ in agreement with the RKKY theory. The order of the transition can be inferred from the sign of the quartic term in Eq. (6). If the quartic term is positive the transition is of second order, while a negative quartic term implies the existence of a first-order phase transition. Using the previous expression for T_c , a first-order transition takes place if

$$\frac{e^2}{\epsilon_0} \frac{1}{\pi} \left(\frac{3\pi^2}{w}\right)^{1/3} \frac{5}{2916} \frac{n_{2D}^{-8/3}}{\left[\frac{7}{30}(S+\frac{1}{2})^4 - \frac{S^2(S+1)^2}{6}\right]} \times \frac{c^2 J^2 S^3 (S+1)^3}{\left(\pi \frac{\hbar^2}{m^*}\right)^3 \left[1 - \frac{m^*}{\hbar^2} \frac{1}{3\pi^2} \frac{e^2}{\epsilon_0} \left(\frac{3\pi^2}{w}\right)^{1/3} n_{2D}^{-2/3}\right]^3} > 1 \quad (8)$$

which implies that for 2D densities lower than $n_{2D}^{\text{first}} \approx 2.1 \times 10^{12} \text{ cm}^{-2}$ the phase transition is of first order ($k_F^{\text{first}} = \sqrt{4\pi n_{2D}^{\text{first}}} = 0.51 \text{ nm}^{-1}$). This estimate is also in good agreement with the LSDA results shown in Fig. 1.

Some comments about the LSDA are in order:

(i) In the HF treatment, the existence of a negative quartic term in the expansion of the exchange energy in powers of ξ is the source for the appearance of first-order phase transitions. In the LSDA, the intermediate spin polarization correlation energy is obtained [13,18–20] by assuming that it has the same polarization dependence as the exchange energy, so that the LSDA expression for E_{xc} also leads to a negative quartic term when expanded in powers of ξ , and a first-order transition is expected. On the other hand, correlation effects [19] weaken the spin dependence of the interaction energy as compared with the results in HF, and we find that the LSDA gives a value for n_{2D}^{first} slightly smaller than that observed in the HF approximation. Numerical evaluation [19] of the partially spin polarized E_{xc} also shows a negative quartic term in the expansion of E_{xc} versus ξ . Hence, we believe that the existence of a first-order phase transition is a *robust* result, independent of the model used for describing the interaction between carriers. Note that a mean field approach, like the one used in this work, is appropriate for the study of first-order transitions, as the correlation length is bounded and spatial fluctuations cannot lead to divergent corrections [21].

(ii) The interpolation formula used for describing the ξ dependence of E_{xc} is not analytic at $\xi = 1$, Eq. (5). This implies that there is, for each pair of values n_{2D} and T , a ξ range near $\xi = 1$ which cannot be reached by minimizing the total free energy. When $\partial \mathcal{F}^2 / \partial \xi^2$ is smaller than zero, the system prefers to be completely spin polarized. More accurate descriptions of the LSDA E_{xc} [19] result in an analytic behavior at $\xi = 1$. Therefore we believe that, in the results shown in Fig. 1, the discontinuous transition which occurs at lower temperatures than the second-order transition T_c is, probably, a spurious result due to the use of a HF-like interpolation for E_{xc} .

We remark again here that the appearance of a first-order transition when decreasing n_{2D} is a real result, not related with the non analyticity of the LSDA expression for E_{xc} .

Now we analyze the effect in the phase diagram of a magnetic field. For $B \neq 0$, the discontinuous transitions shown in Fig. 1 are changed into transitions between phases with two different polarizations, Fig. 2. General thermodynamic arguments show that this line of first-order transitions should end in a critical point, in an analogous way to the liquid-vapor phase diagram. This critical point belongs to the Ising universality class. In the present calculations, the first-order transition persists at all B . This is due to the nonanalyticity of the exchange energy at $\xi = 1$. We expect that a more accurate description of E_{xc} will lead to a critical value of the field beyond which no sharp transition is observed. This is the generic picture expected in transitions between two phases with the same symmetries, like the liquid-vapor transition [21]. Finite temperature effects in the hole gas, not taken into account here, should also weaken the ξ dependence of the free energy, leading to the existence of a critical point.

The existence of discontinuous transitions leads to the possibility of phase separation. The Maxwell construction [21] gives the region where two coexisting phases of

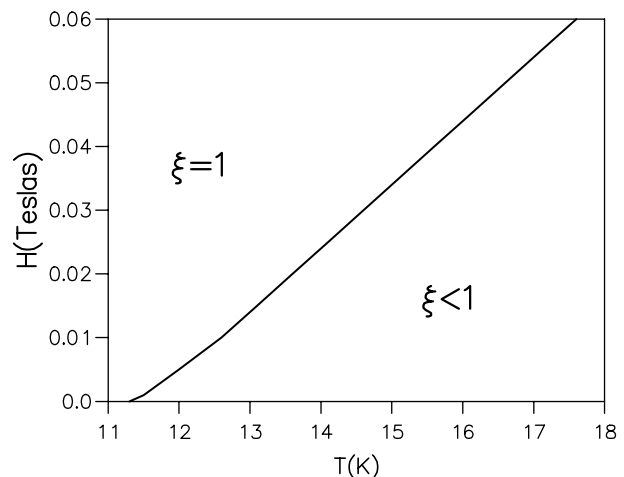


FIG. 2. Phase diagram of a DMS quantum well as a function of T and magnetic field for a hole density such that $k_F = 0.2 \text{ nm}^{-1}$. The line separating the fully polarized from the partially polarized system represents a first-order transition.

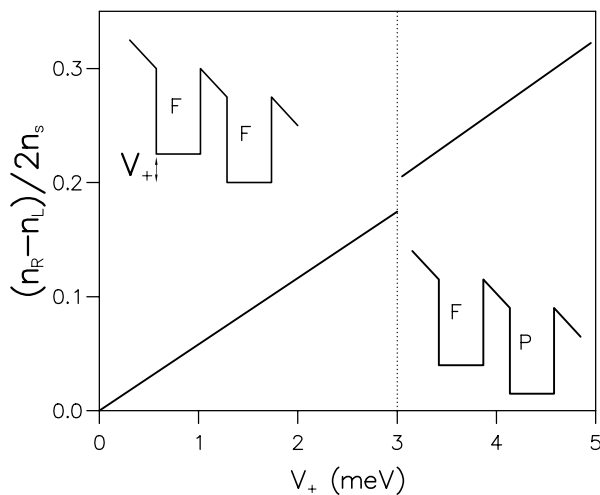


FIG. 3. Charge transfer in a bilayer as a function of the applied voltage V_+ . $n_{L(R)}$ represents the charge in the left (right) well. The width of the wells is $w = 100 \text{ \AA}$ and the barriers are 10 \AA thick. The total areal density is $n_s = 6 \times 10^{11} \text{ cm}^{-2}$ and $T = 10 \text{ K}$. At small V_+ both wells are ferromagnetic, and, by increasing the voltage, there is a transfer of charge from the left to the right well. The jump in the charge transfer occurs when the density in the right well is high enough so that the right well becomes paramagnetic.

different densities are energetically favored, and we find a region of phase separation near the line of first-order transitions. As the two phases are charged, we need to include electrostatic effects. The simplest situation where phase separation can be observed is in a bilayer (the dependence of magnetic couplings on applied field in a bilayer was considered in [22]). Let us imagine two wells with nominal 2D density of holes n_0 . At the temperatures and fields where the first-order transition occurs, there are two phases with the same free energies, $\mathcal{F}_1(n_0) = \mathcal{F}_2(n_0)$. The chemical potential of these two phases differ at this point, and we define $\Delta\mu = \mu_1 - \mu_2$. This difference in chemical potentials will induce a transfer of charge between the two layers, δn , until $\Delta\mu$ is compensated by the induced electrostatic potential, $V \approx e^2 \delta n d / \epsilon_0$, where d is the distance between the layers. Thus, we obtain $\delta n \approx \Delta\mu \epsilon_0 / e^2 d$. For reasonable values of $d \sim 10\text{--}50 \text{ nm}$, we find that the charge transfer is small, $\delta n / n_0 \sim 10^{-2}$. The change in the electrostatic barrier $V \approx \Delta\mu$ is, however, comparable to the Fermi energy and can change significantly the transport properties. All these energies are of the order of a few meV.

In a bilayer system, the first-order transitions analyzed here can be induced by an applied electric field. The field induces a difference in the chemical potential of the two layers, which leads to a charge transfer. By suitably tuning the parameters, the density in one of the layers will reach the value at which the first-order transition discussed above takes place. At this point, there will be an abrupt change in the charge transfer, which can be measured with standard capacitive techniques [14,15]. The charge transfer

as function of electric field, for reasonable parameters, is shown in Fig. 3.

In conclusion, we have analyzed the possible discontinuous transitions in 2D diluted magnetic semiconductors, where a single subband is occupied [23]. We find that the interaction between carriers can lead to first-order transitions in quantum wells. At the transition, the holes become fully polarized. This transition can be induced by a change in the density of the hole gas, the temperature, a magnetic field, and, in multilayer systems, an applied electric field. At these transitions, the minority spin band becomes empty, and the density of states at the Fermi level is reduced by one half. In double layer systems, significant electrostatic barriers can appear near the transition. This change can alter significantly the transport properties [24]. Thus, it can be important in the operation of devices made with these materials.

L. B. thanks A. H. MacDonald, C. Tejedor and A. Rubio for helpful discussions. We acknowledge financial support from Grants No. PB96-0875 and No. PB96-0085 (MEC, Spain) and Grants No. 07N/0045/98 and No. 07N/0027/99) (C. Madrid).

- [1] See, e.g., G. A. Prinz, *Science* **282**, 1660 (1998).
- [2] H. Ohno, *J. Magn. Magn. Mater.* **200**, 110 (1999); *Science* **281**, 951 (1998).
- [3] T. Dietl *et al.*, *Phys. Rev. B* **55**, R3347 (1997).
- [4] F. Matsukara *et al.*, *Phys. Rev. B* **57**, 2037 (1998).
- [5] T. Jungwirth *et al.*, *Phys. Rev. B* **59**, 9818 (1999).
- [6] B. Lee *et al.*, *Phys. Rev. B* **61**, 15 606 (2000).
- [7] Y. Shimikawa *et al.*, *Nature (London)* **379**, 53 (1996).
- [8] J. A. Alonso *et al.*, *Phys. Rev. Lett.* **82**, 189 (1999).
- [9] F. Guinea *et al.*, *Phys. Rev. B* **62**, 391 (2000).
- [10] P. Majumdar *et al.*, *Phys. Rev. Lett.* **81**, 1314 (1998); M. J. Calderón *et al.*, *Phys. Rev. B* **62**, 3368 (2000).
- [11] L. Zheng *et al.*, *Phys. Rev. B* **55**, 4506 (1997).
- [12] I. P. Smorchkova *et al.*, *Physica (Amsterdam)* **249–251B**, 676 (1998).
- [13] S. H. Vosko *et al.*, *Can. J. Phys.* **58**, 1200 (1980).
- [14] J. P. Eisenstein *et al.*, *Phys. Rev. Lett.* **68**, 674 (1992); *Phys. Rev. B* **50**, 1760 (1994).
- [15] S. Ilani *et al.*, preprint cond-mat/9910116.
- [16] Note that for densities of the order of 10^{12} cm^{-2} the Fermi energy of the spin polarized hole gas is near 500 K.
- [17] E. K. U. Gross, E. Runge, and O. Heinonen, in *Many-Particle Theory* (Hilger, Bristol, 1991).
- [18] U. von Barth and L. Hedin, *J. Phys. C* **5**, 1629 (1972).
- [19] O. Gunnarson *et al.*, *Phys. Rev. B* **13**, 4274 (1976).
- [20] J. P. Perdew and A. Zunger, *Phys. Rev. B* **23**, 5048 (1981).
- [21] K. Huang, *Statistical Mechanics* (Wiley, New York, 1987).
- [22] L. G. Ferreira *et al.*, *Semicond. Sci. Technol.* **12**, 1592 (1997).
- [23] When higher subbands begin to fill, we expect a more complicated phase diagram, see M. A. Boselli *et al.*, *J. Appl. Phys.* **87**, 6439 (2000).
- [24] J. C. Egues, *Phys. Rev. Lett.* **80**, 4578 (1998).